

Correspondence

Low-Complexity MIMO Detection Based on Post-Equalization Subspace Search

Ronald Y. Chang and Wei-Ho Chung, *Member IEEE*

Abstract—Two low-complexity effective detection schemes for multiple-input-multiple-output (MIMO) systems based on post-equalization subspace search are proposed in this paper. With the initial solution given by the linear detector, calibrated constellation search is conducted in symbol subspace and eigenspace associated with the largest estimation errors in linear detection to identify improved solutions. Complexity analysis is performed to understand the cost of the proposed add-on procedures. Simulation results demonstrate that the proposed schemes yield noticeable performance gains over linear detectors at moderate additional computational cost.

Index Terms—Linear detection, low-complexity detection, multiple-input-multiple-output (MIMO) systems.

I. INTRODUCTION

Multiple-input-multiple-output (MIMO) technology has the potential to greatly enhance the capacity of wireless cellular networks and/or the reliability of data transmission through wireless media. It has been adopted in advanced cellular systems such as Long Term Evolution Advanced (LTE-A) [1]. To fully exploit the potential of MIMO, a high-fidelity and low-complexity detection scheme at the receiving end is needed. Maximum-likelihood (ML) detection is known to be theoretically optimal but computationally infeasible in practice. While various reduced-complexity optimal or near-optimal algorithms have been proposed [2], [3], their worst-case complexity is still formidably high for real-time implementation [4].

The well-known linear zero-forcing (ZF) and minimum-mean-square-error (MMSE) detection presents an attractive low-complexity option for practical use with suboptimal performance. Applications of the ZF or MMSE criterion have been examined in many contexts, such as sphere decoding [5], lattice-reduction-aided detection [6], successive interference cancellation (SIC)-based detection [7]–[9], reduced-dimension ML search-based decoding [10], and iterative detection for coded systems [11]. This work specifically deals with the standard ZF or MMSE detector and augments it with a novel low-complexity add-on procedure. We introduce the concept of post-equalization constellation search for the augmentation, aiming to leverage the performance of linear detection in well-conditioned channels and “correct” its errors in ill-conditioned channels [12]. Constellation search is conducted in sensibly selected signal subspaces after linear detection. Two novel

Manuscript received February 12, 2011; revised May 15, 2011, August 4, 2011, and October 3, 2011; accepted October 19, 2011. Date of publication October 26, 2011; date of current version January 20, 2012. This work was supported in part by the National Science Council of Taiwan under Grant NSC 100-2221-E-001-004 and in part by the Industrial Technology Research Institute of Taiwan under the Ministry of Economic Affairs project. The review of this paper was coordinated by Dr. X. Dong.

R. Y. Chang and W.-H. Chung (Corresponding author) are with the Research Center for Information Technology Innovation, Academia Sinica, Taipei 115, Taiwan (e-mail: yjrchang@gmail.com; whc@citi.sinica.edu.tw).

Color versions of one or more of the figures in this paper are available online at <http://ieeexplore.ieee.org>.

Digital Object Identifier 10.1109/TVT.2011.2173703

algorithms that establish the “search-and-correct” procedure in symbol subspace and eigenspace, respectively, are proposed. Performance and complexity results demonstrate that the proposed schemes offer notable performance advantage over conventional linear detectors. The pros and cons of the two proposed algorithms in different MIMO system settings are also discussed.

This paper is organized as follows: Section II defines the system model and reviews linear detection. Our proposed methods are described in Section III. Complexity evaluation of various detection algorithms is conducted in Section IV. Numerical figures of the complexity and the performance are demonstrated in Section V. Finally, concluding remarks are given in Section VI.

II. SYSTEM DESCRIPTION AND REVIEW OF LINEAR DETECTION

A. System Model and Problem Description

We consider a MIMO transmission system with M transmit antennas and N receive antennas ($N \geq M$). Then, the baseband signal model is given by

$$\mathbf{y} = \mathbf{H}\tilde{\mathbf{x}} + \mathbf{n} \quad (1)$$

where \mathbf{y} is the $N \times 1$ received signal composed of $M \times 1$ transmitted signal $\tilde{\mathbf{x}}$ passed through $N \times M$ flat-fading channel \mathbf{H} and $N \times 1$ perturbing noise vector \mathbf{n} . Transmitted symbol vector $\tilde{\mathbf{x}}$ contains uncorrelated entries from the countably finite set of modulation constellation points, denoted by \mathbb{S} , and has zero mean and covariance matrix $\sigma_x^2 \mathbf{I}_M$, where \mathbf{I}_M is the $M \times M$ identity matrix. Complex-valued channel matrix \mathbf{H} has independent and identically distributed (i.i.d.) Gaussian entries with zero mean and covariance matrix $\sigma_H^2 \mathbf{I}_N$, where $\sigma_H^2 = 1$. The channel information is assumed perfectly known to the receiver. Noise \mathbf{n} is additive white Gaussian noise (AWGN) with i.i.d. complex elements and has zero mean and covariance matrix $\sigma_n^2 \mathbf{I}_N$.

Given the signal model in (1), ML detection is equivalent to solving a constrained least-squares problem, i.e.,

$$\tilde{\mathbf{x}}_{\text{ML}} = \arg \min_{\mathbf{x} \in \mathbb{S}^M} D_{\mathbf{x}} \quad (2)$$

where $D_{\mathbf{x}} \triangleq \|\mathbf{y} - \mathbf{H}\mathbf{x}\|^2$ is the *likelihood metric* for some \mathbf{x} given \mathbf{y} and \mathbf{H} , and $\|\cdot\|$ is the l_2 -norm of a vector. ML detection is optimal in the sense that it finds a solution that minimizes the error probability given equally probable transmitted symbol vectors. However, its search space quickly grows prohibitively large for moderate-sized M and $|\mathbb{S}|$ for ML detection to be computationally feasible in practice, where $|\cdot|$ denotes the cardinality of a set. As a result, some suboptimal detection schemes with low complexity are useful in practical systems.

B. Linear ZF and MMSE Detection

Two commonly used suboptimal detection schemes with very low complexity are ZF and MMSE detection. ZF detection performs linear equalization on the received symbol vector \mathbf{y} followed by entrywise quantization (or slicing) to the closest constellation point. Its equalization matrix is given by the Moore–Penrose pseudoinverse [13] of \mathbf{H} , i.e.,

$$\mathbf{G}_{\text{ZF}} = (\mathbf{H}^H \mathbf{H})^{-1} \mathbf{H}^H \quad (3)$$

where $(\cdot)^{-1}$ and $(\cdot)^H$ denote matrix inverse and Hermitian matrix transpose, respectively. It is assumed that \mathbf{H} has full column rank. Equalized symbol vector $\tilde{\mathbf{x}}_{\text{ZF}}$ is given by

$$\tilde{\mathbf{x}}_{\text{ZF}} = \mathbf{G}_{\text{ZF}}\mathbf{y} = \tilde{\mathbf{x}} + \tilde{\mathbf{n}} \quad (4)$$

where $\tilde{\mathbf{n}} = \mathbf{G}_{\text{ZF}}\mathbf{n}$. The ZF-detected symbol vector is $\tilde{\mathbf{x}}_{\text{ZF}} = q(\tilde{\mathbf{x}}_{\text{ZF}})$, where $q(\cdot)$ denotes entrywise quantization.

MMSE detection follows the same procedure but with a different equalization matrix, which was derived from minimizing mean-square error $\text{E}[\|\mathbf{G}\mathbf{y} - \tilde{\mathbf{x}}\|^2]$ and given by [14]

$$\mathbf{G}_{\text{MMSE}} = \left(\mathbf{H}^H\mathbf{H} + \frac{\sigma_n^2}{\sigma_x^2}\mathbf{I}_M \right)^{-1} \mathbf{H}^H. \quad (5)$$

It follows that the equalized symbol vector is

$$\tilde{\mathbf{x}}_{\text{MMSE}} = \mathbf{G}_{\text{MMSE}}\mathbf{y} = \hat{\mathbf{x}} + \hat{\mathbf{n}} \quad (6)$$

where $\hat{\mathbf{x}} = \mathbf{G}_{\text{MMSE}}\mathbf{H}\tilde{\mathbf{x}}$, and $\hat{\mathbf{n}} = \mathbf{G}_{\text{MMSE}}\mathbf{n}$. The MMSE-detected symbol vector is $\tilde{\mathbf{x}}_{\text{MMSE}} = q(\tilde{\mathbf{x}}_{\text{MMSE}})$. Note that, different from ZF detection in (4), MMSE detection trades complete interference nullification for the mitigation of noise enhancement in (6).

III. PROPOSED DETECTION ALGORITHMS

Equalization-based detection methods generally achieve significantly lower computational complexity compared with ML detection at the cost of suboptimal performance. To improve the performance of equalization-based methods while still maintaining their low-complexity advantage, we propose two efficient schemes that perform intelligent post-equalization constellation search in symbol subspace and eigenspace, respectively, without introducing a substantial complexity increase. The proposed two schemes can work in conjunction with ZF or MMSE detection, as individually described as follows.

A. ZF Detection Plus Symbol Subspace Search (ZF-SS)

The first proposed scheme is developed based on the observation that linear detectors provide satisfactory initial solutions for well-conditioned channels, and thus, a reduced-dimension exhaustive search in selected symbol subspace may correct symbol errors incurred in linear equalization and yield a better solution. Specifically, this post-equalization search is conducted in K -dimensional symbol subspace ($1 \leq K \leq M$), and among the $\binom{M}{K}$ possible subspaces, we choose the one that corresponds to the K most error-prone symbols. If ZF detection was employed, these are symbols with a low postdetection signal-to-noise ratio (SNR), which, from (4), are symbols associated with rows $\mathbf{g}_{\text{ZF}}^{(i)}$ of \mathbf{G}_{ZF} that have large l_2 -norm. These K symbols in $\tilde{\mathbf{x}}_{\text{ZF}}$ are replaced by different combinations in \mathbb{S}^K to identify improved solutions. When $K = M$, this method is equivalent to ML detection; therefore, for low-complexity considerations, usually, $K = 1$ or $K = 2$ is used. The ZF-SS algorithm is summarized as follows.

Algorithm I: ZF-SS(K)

- Step 1) Calculate $\tilde{\mathbf{x}}_{\text{ZF}} = [\tilde{x}_{\text{ZF}}^1, \dots, \tilde{x}_{\text{ZF}}^M]^T$ and $\|\mathbf{g}_{\text{ZF}}^{(i)}\|$, $i = 1, \dots, M$.
- Step 2) Order elements of $\tilde{\mathbf{x}}_{\text{ZF}}$ in descending order of $\|\mathbf{g}_{\text{ZF}}^{(i)}\|$, resulting in $\tilde{\mathbf{x}}_{\text{ZF}}^{(P)} = [\tilde{x}_{\text{ZF}}^{i_1}, \dots, \tilde{x}_{\text{ZF}}^{i_M}]^T$, where $\mathbf{i} = [i_1, \dots, i_M]^T$ denotes the new indexing after ordering.
- Step 3) Obtain the set of all search candidates $\Psi_{\text{SS}} = \{[x^{i_1}, \dots, x^{i_K}, \tilde{x}_{\text{ZF}}^{i_{K+1}}, \dots, \tilde{x}_{\text{ZF}}^{i_M}]^T \mid [x^{i_1}, \dots, x^{i_K}]^T \in \mathbb{S}^K\}$.
- Step 4) Output the solution $\tilde{\mathbf{x}}_{\text{ZF-SS}(K)} = \arg \min_{\mathbf{x} \in \Psi_{\text{SS}}} D_{\mathbf{x}}$.

B. MMSE-SS

The ZF-SS approach translates to MMSE-SS with one twist. As shown in (6), the MMSE-equalized symbol contains both interference and noise, and thus, the signal-to-interference-plus-noise ratio rather than the SNR should be considered in symbol selection. More specifically, first note that (6) can be rewritten as [8]

$$\tilde{\mathbf{x}}_{\text{MMSE}} = (\mathbf{H}^H\mathbf{H})^{-1}\mathbf{H}^H\mathbf{y} = \mathbf{G}_{\text{MMSE}}\mathbf{y} \quad (7)$$

where

$$\mathbf{H} = \begin{bmatrix} \mathbf{H} \\ \frac{\sigma_n}{\sigma_x}\mathbf{I}_M \end{bmatrix}, \quad \mathbf{y} = \begin{bmatrix} \mathbf{y} \\ \mathbf{0}_{M,1} \end{bmatrix}. \quad (8)$$

Then, symbols associated with rows $\mathbf{g}_{\text{MMSE}}^{(i)}$ of \mathbf{G}_{MMSE} that have large l_2 -norm are selected for correction. As a result, replacing $\tilde{\mathbf{x}}_{\text{ZF}}$ by $\tilde{\mathbf{x}}_{\text{MMSE}}$ and $\mathbf{g}_{\text{ZF}}^{(i)}$ by $\mathbf{g}_{\text{MMSE}}^{(i)}$ in Algorithm I gives the MMSE-SS algorithm. Note that, since \mathbf{G}_{MMSE} comprises the first N columns of \mathbf{G}_{MMSE} , selection based on rows of \mathbf{G}_{MMSE} is suboptimal.

C. ZF Detection Plus Eigenspace Search (ZF-ES)

The second proposed scheme conducts a similar post-equalization search but in a different subspace. It is motivated by the fact that the error covariance matrix for ZF detection, i.e., $\Phi_{\text{ZF}} = \text{E}[(\tilde{\mathbf{x}}_{\text{ZF}} - \tilde{\mathbf{x}})(\tilde{\mathbf{x}}_{\text{ZF}} - \tilde{\mathbf{x}})^H]$, is equal to the covariance matrix of colored Gaussian noise $\tilde{\mathbf{n}}$, i.e., $\mathbf{R}_{\tilde{\mathbf{n}}} = \sigma_n^2(\mathbf{H}^H\mathbf{H})^{-1}$. Since small eigenvalues of $\mathbf{H}^H\mathbf{H}$ will lead to large estimation errors and the corresponding eigenvectors align with directions where color noise $\tilde{\mathbf{n}}$ exhibits large variance, a post-equalization search is initiated in the eigenspace constructed by these eigenvectors to correct the most likely errors incurred in linear detection due to noise perturbation. The detailed procedure is described as follows.

1) *Search Directions*: To obtain the search directions, we first perform singular value decomposition (SVD) on channel matrix \mathbf{H} , i.e.,

$$\mathbf{H} = \mathbf{U}\mathbf{\Sigma}\mathbf{V}^H \quad (9)$$

where \mathbf{U} and \mathbf{V} are $N \times N$ and $M \times M$ unitary matrices, and $\mathbf{\Sigma}$ is an $N \times M$ diagonal matrix with positive-valued singular values $\varsigma_1 \leq \varsigma_2 \leq \dots \leq \varsigma_M$ on the diagonal (since $N \geq M$ and \mathbf{H} has full rank). Then, substituting (9) into $\mathbf{R}_{\tilde{\mathbf{n}}}$ yields

$$\mathbf{R}_{\tilde{\mathbf{n}}} = \sigma_n^2(\mathbf{H}^H\mathbf{H})^{-1} = \mathbf{V}\mathbf{\Omega}_1\mathbf{V}^H \quad (10)$$

where $\mathbf{\Omega}_1 = \sigma_n^2(\mathbf{\Sigma}^H\mathbf{\Sigma})^{-1}$ is an $M \times M$ diagonal matrix with $\sigma_n^2/\varsigma_1^2 \geq \sigma_n^2/\varsigma_2^2 \geq \dots \geq \sigma_n^2/\varsigma_M^2$ on the diagonal. Since the first few columns of \mathbf{V} , denoted by $\mathbf{v}_1, \mathbf{v}_2, \dots$, are eigenvectors that correspond to large eigenvalues of $\mathbf{R}_{\tilde{\mathbf{n}}}$, or equivalently, small eigenvalues of $\mathbf{H}^H\mathbf{H}$, they indicate the directions in which the proposed search is conducted. Let L be the *dimension* ($1 \leq L \leq M$) and $\mathbf{v}_1, \mathbf{v}_2, \dots, \mathbf{v}_L$ be the *principal directions* of the search. Then, ES with dimension L is established in the M -dimensional symbol hyperspace in principal directions $\mathbf{v}_1, \mathbf{v}_2, \dots, \mathbf{v}_L$ and their reverse directions away from ZF-equalized symbol vector $\tilde{\mathbf{x}}_{\text{ZF}}$. An illustrative example for $L = 2$ is shown in Fig. 1.

2) *Search Steps*: In each search direction, the search range is chosen to cover the extent to which $\tilde{\mathbf{x}}_{\text{ZF}}$ was (most likely) deviated from $\tilde{\mathbf{x}}$, and the search step size is chosen such that it is neither too fine (unnecessarily higher complexity) nor too coarse (risk of skipping constellation points). It turns out that a sensible choice of the search step size is d , which is the distance between two nearest constellation points in \mathbb{S} , and a reasonable choice of the search range is one that

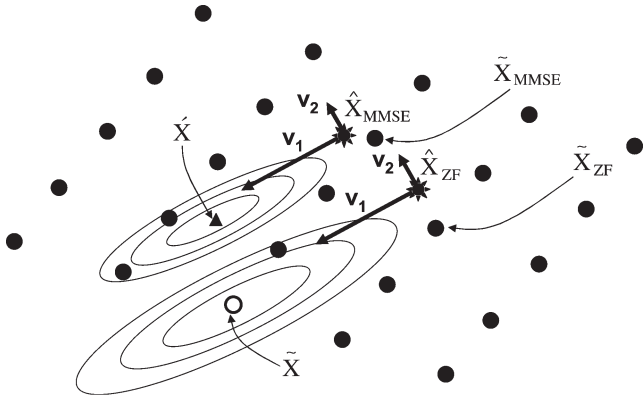


Fig. 1. Illustration of the ES method. Each lattice point represents a possible \mathbf{x} in the M -dimensional hyperspace, with the unfilled one being the actually transmitted symbol $\tilde{\mathbf{x}}$. Concentric disks depict contour lines of the pdf of $\hat{\mathbf{x}}_{\text{ZF}}$ and $\hat{\mathbf{x}}_{\text{MMSE}}$, which are $\tilde{\mathbf{x}}$ and $\tilde{\mathbf{x}}$ perturbed by colored Gaussian noise $\tilde{\mathbf{n}}$ and $\hat{\mathbf{n}}$, respectively. Searching away from $\hat{\mathbf{x}}_{\text{ZF}}$ and $\hat{\mathbf{x}}_{\text{MMSE}}$ in principal directions \mathbf{v}_1 and \mathbf{v}_2 and their reverse directions increases the chance of finding the actually transmitted symbol $\tilde{\mathbf{x}}$.

covers most of the noise power in each direction. More specifically, the set of search steps along \mathbf{v}_i in relation to $\hat{\mathbf{x}}_{\text{ZF}}$ at the origin is given by

$$\mathbb{B}_i = \{0, \pm d, \pm 2d, \dots, \pm \alpha_i d\}, \quad i = 1, \dots, L \quad (11)$$

where $\alpha_i = \lceil (3\sigma_n/\zeta_i)/d \rceil$, and $\lceil \cdot \rceil$ is the ceiling function. That is, the search range covers three standard deviations of the noise away from the origin. Note that $|\mathbb{B}_1| \geq |\mathbb{B}_2| \geq \dots \geq |\mathbb{B}_L|$.

As will be shown in Section V, $L = 1$ is observed to be sufficient to yield satisfactory performance in the simulated MIMO settings as additional dimensions contribute little performance gain at more computational cost. The ZF-ES algorithm is summarized as follows.

Algorithm II: ZF-ES(L)

- Step 1) Calculate $\hat{\mathbf{x}}_{\text{ZF}}$ and \mathbf{v}_i , ζ_i , $i = 1, \dots, L$.
- Step 2) Obtain the set of search steps along \mathbf{v}_i , \mathbb{B}_i , $i = 1, \dots, L$.
- Step 3) Obtain the set of all search candidates $\Psi_{\text{ES}} = \{q(\hat{\mathbf{x}}_{\text{ZF}} + \sum_{i=1}^L b_i \mathbf{v}_i) | \forall b_i \in \mathbb{B}_i, i = 1, \dots, L\}$.
- Step 4) Output the solution $\hat{\mathbf{x}}_{\text{ZF-ES}(L)} = \arg \min_{\mathbf{x} \in \Psi_{\text{ES}}} D_{\mathbf{x}}$.

D. MMSE-ES

For the ES algorithm to work in conjunction with an MMSE detector, first note that the error covariance matrix for MMSE detection, i.e., $\Phi_{\text{MMSE}} = \mathbb{E}[(\hat{\mathbf{x}}_{\text{MMSE}} - \tilde{\mathbf{x}})(\hat{\mathbf{x}}_{\text{MMSE}} - \tilde{\mathbf{x}})^H]$, is given by $\sigma_n^2 (\mathbf{H}^H \mathbf{H} + (\sigma_n^2/\sigma_x^2) \mathbf{I}_M)^{-1}$ [8]. Therefore, similar to ZF detection, small eigenvalues of $\mathbf{H}^H \mathbf{H}$ will lead to large estimation errors in MMSE detection. Moreover, the eigenvectors corresponding to small eigenvalues of $\mathbf{H}^H \mathbf{H}$ align with directions where color noise $\tilde{\mathbf{n}}$ exhibits large variance, as the covariance matrix of $\tilde{\mathbf{n}}$ is given by

$$\begin{aligned} \mathbf{R}_{\tilde{\mathbf{n}}} &= \sigma_n^2 \left(\mathbf{H}^H \mathbf{H} + \frac{\sigma_n^2}{\sigma_x^2} \mathbf{I}_M \right)^{-1} \mathbf{H}^H \mathbf{H} \left(\mathbf{H}^H \mathbf{H} + \frac{\sigma_n^2}{\sigma_x^2} \mathbf{I}_M \right)^{-H} \\ &= \mathbf{V} \mathbf{\Omega}_2 \mathbf{V}^H \end{aligned} \quad (12)$$

where $\mathbf{\Omega}_2$ is an $M \times M$ diagonal matrix with $\sigma_n^2 \zeta_i^2 (\zeta_i^2 + (\sigma_n^2/\sigma_x^2))^{-2}$, $i = 1, \dots, M$, on the diagonal. Comparing (10) and (12), it is shown that the search directions for ZF-ES can be readopted for MMSE-ES (as shown in Fig. 1), however, with a smaller search range needed for MMSE-ES since $\zeta_i^2 (\zeta_i^2 + (\sigma_n^2/\sigma_x^2))^{-2} \leq \zeta_i^{-2}$. For

simplicity, we consider the same search range and steps for MMSE-ES (which somewhat trades the complexity for performance). Therefore, replacing $\hat{\mathbf{x}}_{\text{ZF}}$ by $\hat{\mathbf{x}}_{\text{MMSE}}$ in Algorithm II gives the MMSE-ES algorithm.

IV. COMPLEXITY EVALUATION

Here, we evaluate the complexity of the proposed schemes. Since the complexity of SS- and ES-based algorithms depends on the number of search candidates (Step 3 in Algorithms I and II), we first examine this quantity analytically and numerically in Section IV-A. Then, we compare our proposed schemes with conventional linear detectors and SIC-based BLAST schemes in terms of complex multiplications and additions in Section IV-B.

A. Number of Search Candidates in SS and ES

It is straightforward to see that the number of search candidates in ZF-SS and MMSE-SS is equal to $|\mathbb{S}|^K$. For ZF-ES and MMSE-ES, however, it requires some analytical exposition. First note that the number of search candidates for ZF-ES and MMSE-ES can be approximated by $\prod_{i=1}^L |\mathbb{B}_i|$ if L dimensions were considered (we get an upper bound by ignoring the fact that $q(\cdot)$ may take two distinct search points to the same search candidate in Ψ_{ES} , in Step 3 of Algorithm II). Since the performance and complexity of the ES-based schemes are dominated by the first dimension (see Section V), in the following, we quantitatively examine $|\mathbb{B}_1|$ and use the result as an upper bound for other dimensions.

Since $|\mathbb{B}_1|$ is a random variable that depends on \mathbf{H} , we are interested in understanding its expected value averaged over all channel realizations. From (11) and using the property of the ceiling function, we directly have

$$|\mathbb{B}_1| < 6 \cdot \left(\frac{\sigma_n}{d} \right) \cdot \delta_1 + 3 \quad (13)$$

where $\delta_1 = 1/\zeta_1$. Note that σ_n and d are fully determined by the system setting and δ_1 is a random variable that depends on the channel. First, we analyze δ_1 using the following result.

Theorem 1 [15]: Let $\tilde{\mathbf{W}}(m, m)$ be a Hermitian $m \times m$ random matrix $\mathbf{A} \mathbf{A}^H$, where \mathbf{A} is an $m \times m$ random matrix with i.i.d. elements whose real and imaginary parts are i.i.d. $\mathcal{N}(0, 1)$. Then, the probability density function (pdf) of the smallest eigenvalue λ_{\min} of $\tilde{\mathbf{W}}(m, m)$ is $f_{\lambda_{\min}}(x) = (m/2)e^{-(m/2)x}$, i.e., it is exponentially distributed with parameter $m/2$.

In our system, $\mathbf{H}^H \mathbf{H}$ is a $1/(2M)\tilde{\mathbf{W}}(M, M)$ matrix. Thus, ζ_1^2 , which is the smallest eigenvalue of $\mathbf{H}^H \mathbf{H}$, is exponentially distributed with pdf given by $f_{\zeta_1^2}(x) = M^2 e^{-M^2 x}$, $x \geq 0$. It follows that ζ_1 is Rayleigh distributed with pdf $f_{\zeta_1}(x) = 2M^2 x e^{-M^2 x^2}$, $x \geq 0$. Then, the pdf of $\delta_1 = 1/\zeta_1$ is derived by using the standard change-of-variable procedure as $f_{\delta_1}(x) = (2M^2/x^3)e^{-(M^2/x^2)}$, $x > 0$. After some algebraic manipulations, it can be shown that $\mathbb{E}[\delta_1] = M\sqrt{\pi}$.

Second, σ_n/d can be specified for different system settings after noting that the SNR, i.e., ϑ , is defined as

$$\begin{aligned} \vartheta &= \frac{\mathbb{E}[\|\mathbf{H}\tilde{\mathbf{x}}\|^2]}{\mathbb{E}[\|\mathbf{n}\|^2]} \\ &= \frac{\mathbb{E}[\tilde{\mathbf{x}}^H \mathbf{H}^H \mathbf{H} \tilde{\mathbf{x}}]}{\mathbb{E}[\mathbf{n}^H \mathbf{n}]} = \frac{NM\sigma_H^2 \mathbb{E}[(\tilde{x}^i)^2]}{N\sigma_n^2} = \frac{M\sigma_x^2}{\sigma_n^2} \end{aligned} \quad (14)$$

where \tilde{x}^i is the i th element of $\tilde{\mathbf{x}}$. With the bit energy of each transmitted symbol normalized to 1, we can obtain σ_x^2/d^2 for different modulations. Thus, σ_n/d can be represented in terms of M and ϑ for

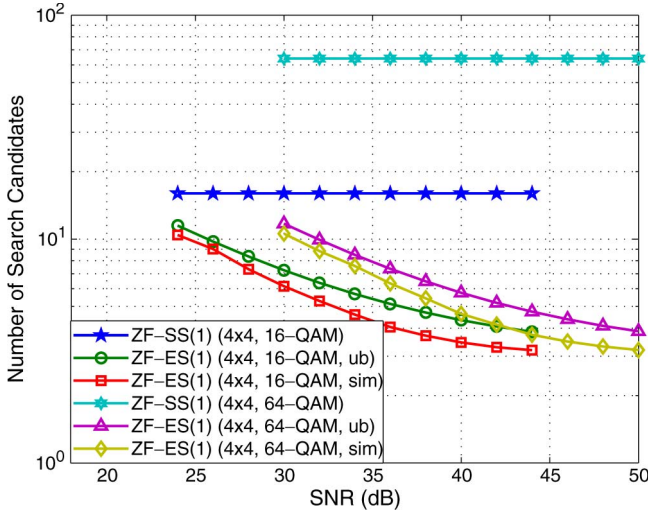


Fig. 2. Number of search candidates in the ZF-SS(1) and ZF-ES(1) algorithms for 4×4 MIMO with 16-QAM and 64-QAM.

different modulations from (14). Collecting these results, and taking expectation on both sides of (13) and substituting $E[\delta_1] = M\sqrt{\pi}$ into it, yield

$$E[|\mathbb{B}_1|] < \sqrt{\beta \frac{\pi M^3}{\vartheta}} + 3 \quad (15)$$

where $\beta = 36(\sigma_x^2/d^2)$, which is equal to 18, 90, and 378 for 4-quadrature amplitude modulation (4-QAM), 16-QAM, and 64-QAM, respectively.

Fig. 2 shows the number of search candidates for ZF-SS and ZF-ES algorithms for 4×4 MIMO with 16-QAM and 64-QAM. For ZF-ES, both the analytical upper bound in (15) and numerical results are shown. The results in Fig. 2 apply to MMSE versions of the algorithms as well, as the number of search candidates does not depend on the initial linear detector. As shown, the ZF-SS scheme has a fixed number of search candidates, which proportionally increases with the order of modulation. In comparison, the ZF-ES scheme has fewer and varying number of search candidates, which moderately increases with the order of modulation. These results suggest that (without taking into account the complexity of other procedures of each algorithm) ES-based algorithms are efficient for high SNRs and high-order modulations, whereas SS-based algorithms are more useful for low-order modulations. This will be further investigated in Section V.

B. Complexity Comparisons

The overall computational complexity of our proposed algorithms in comparison to conventional methods is evaluated here. For simplicity, we consider an equal number of transmit and receive antennas, i.e., $M = N$. Since all processing is conducted on complex values as given by the signal model in (1), all the calculations below refer to complex operations.

The computations of ZF and MMSE detection in (4) and (6) involve computing a matrix inverse and some matrix/vector multiplications. We first compute $\mathbf{H}^H \mathbf{H}$ and $\mathbf{H}^H \mathbf{H} + (\sigma_n^2/\sigma_x^2)\mathbf{I}_M$ by direct multiplications and accumulations, which require $(1/2)M^3 + (1/2)M^2$ multiplications and $(1/2)M^3 - (1/2)M$ additions, and $(1/2)M^3 + (1/2)M^2$ multiplications and $(1/2)M^3 + (1/2)M$ additions, respectively. Then, we compute the inverse of the two matrices by the efficient LDL^H decomposition

method [7], which requires $(1/2)M^3 + (1/2)M^2 - M$ multiplications and $(1/2)M^3 - (1/2)M^2$ additions. Summing up these numbers plus some additional computations required for matrix/vector multiplications, the overall complexity of ZF and MMSE detection is given by $M^3 + 3M^2 - M$ multiplications and $M^3 + (3/2)M^2 - (5/2)M$ additions, and $M^3 + 3M^2 - M$ multiplications and $M^3 + (3/2)M^2 - (3/2)M$ additions, respectively.

The overall complexity of the ZF-SS algorithm includes the complexity of ZF detection, computing the l_2 -norm for rows of \mathbf{G}_{ZF} (M^2 multiplications and $M^2 - M$ additions), and computing D_x ($M^2 + M$ multiplications and $M^2 + M - 1$ additions) for each search candidate. Summing these up, the ZF-SS(K) algorithm requires $M^3 + (|\mathbb{S}^K + 4)M^2 + (|\mathbb{S}^K - 1)M$ multiplications and $M^3 + (|\mathbb{S}^K + (5/2))M^2 + (|\mathbb{S}^K - (7/2))M - |\mathbb{S}^K$ additions. For MMSE-SS, the complexity involves MMSE equalization based on (7) ($(3/2)M^3 + (7/2)M^2 - M$ multiplications and $(3/2)M^3 + 2M^2 - (5/2)M$ additions), calculating the l_2 -norm for rows of \mathbf{G}_{MMSE} ($2M^2$ multiplications and $2M^2 - M$ additions), and computing D_x for each search candidate. Overall, the MMSE-SS(K) algorithm requires $(3/2)M^3 + (|\mathbb{S}^K + (11/2))M^2 + (|\mathbb{S}^K - 1)M$ multiplications and $(3/2)M^3 + (|\mathbb{S}^K + 4)M^2 + (|\mathbb{S}^K - (7/2))M - |\mathbb{S}^K$ additions.

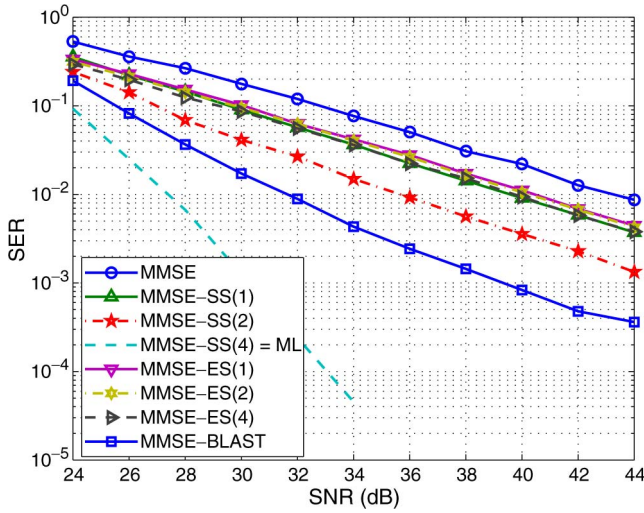
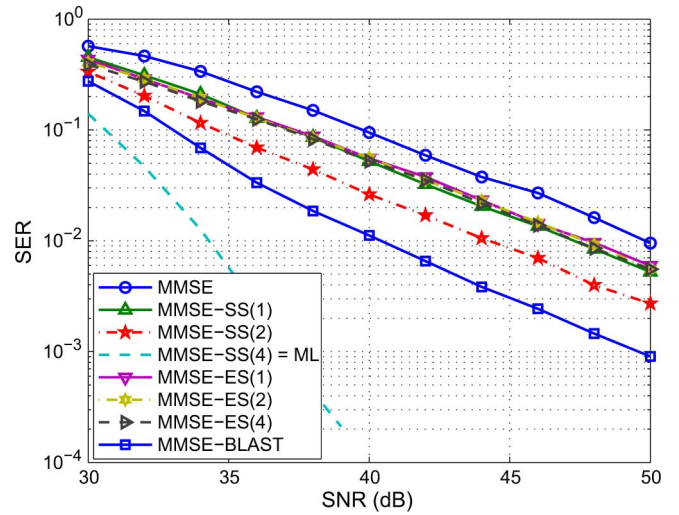
The overall complexity of the ZF-ES algorithm, in general, includes the complexity of ZF detection, performing SVD of \mathbf{H} , and computing D_x for each search candidate. The complexity of performing SVD using the Golub-Reinsch algorithm to get $\mathbf{\Sigma}$ and \mathbf{V} in (9) is $12M^3$, which includes approximately equal numbers of multiplications and additions [13]. If only 1-D ES was performed ($L = 1$), the power method can be used to compute the dominant (largest) eigenvalue and eigenvector of $(\mathbf{H}^H \mathbf{H})^{-1}$ with lower complexity on the order of $\mathcal{O}(4kM^2 + 3kM)$ if k iterations are taken [16]. Therefore, the ZF-ES(L), $L > 1$ algorithm requires $7M^3 + (\rho_L + 3)M^2 + (\rho_L - 1)M$ multiplications and $7M^3 + (\rho_L + (3/2))M^2 + (\rho_L - (5/2))M - \rho_L$ additions, where $\rho_L = E[\sum_{i=1}^L |\mathbb{B}_i|]$. The ZF-ES(1) algorithm requires $M^3 + (\rho_1 + 5)M^2 + (\rho_1 + (1/2))M$ multiplications and $M^3 + (\rho_1 + (7/2))M^2 + (\rho_1 - 1)M - \rho_1$ additions, where we have assumed equal numbers of multiplications and additions in the complexity of the power method approximated by $4M^2 + 3M$. For the MMSE-ES algorithm, note that the same power method can be applied on $(\mathbf{H}^H \mathbf{H} + (\sigma_n^2/\sigma_x^2)\mathbf{I}_M)^{-1}$ to obtain the dominant eigenvalue and eigenvector that are needed. Therefore, simply by replacing ZF with MMSE detection and reworking the complexity accordingly, we obtain the computation counts: the MMSE-ES(L), $L > 1$ algorithm requires $7M^3 + (\rho_L + 3)M^2 + (\rho_L - 1)M$ multiplications and $7M^3 + (\rho_L + (3/2))M^2 + (\rho_L - (3/2))M - \rho_L$ additions, and the MMSE-ES(1) algorithm requires $M^3 + (\rho_1 + 5)M^2 + (\rho_1 + (1/2))M$ multiplications and $M^3 + (\rho_1 + (7/2))M^2 + \rho_1 M - \rho_1$ additions.

The V-BLAST algorithm with optimal-ordered SIC detection based on the ZF/MMSE criterion [17], termed ZF/MMSE-BLAST in this paper, is an efficient low-complexity detection scheme adopted here for comparison with our proposed methods. The complexity of the traditional MMSE-BLAST is $(43/12)M^4 + (22/3)M^3 + (65/12)M^2 - (1/3)M$ multiplications and $(43/12)M^4 + (20/3)M^3 + (53/12)M^2 - (5/3)M$ additions [18].¹ Table I summarizes the complexity results presented here.

¹Improved algorithms to the traditional V-BLAST method exist, which somewhat reduce these numbers, but the difference in the case of small numbers of transmit and receive antennas (e.g., $M = 4$ or 8) is slight. See [18] for details.

TABLE I
 COMPLEXITY COMPARISONS OF MIMO DETECTION SCHEMES IN TERMS OF NUMBER OF MULTIPLICATIONS AND ADDITIONS

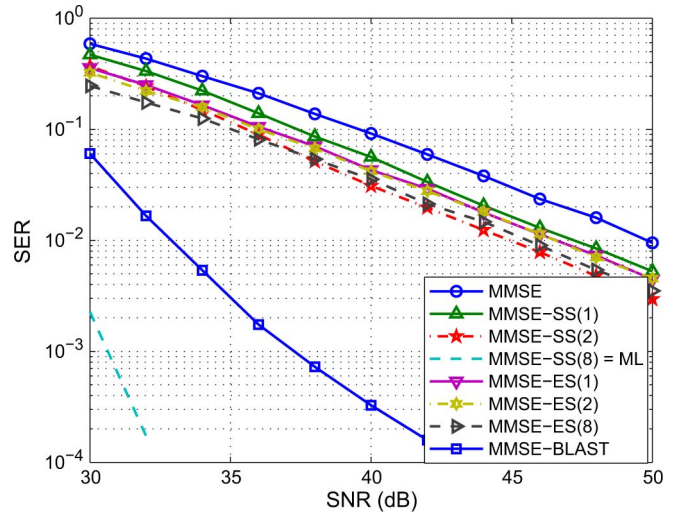
Detection Schemes	Number of Multiplications	Number of Additions
ZF	$M^3 + 3M^2 - M$	$M^3 + \frac{3}{2}M^2 - \frac{5}{2}M$
MMSE	$M^3 + 3M^2 - M$	$M^3 + \frac{3}{2}M^2 - \frac{3}{2}M$
ZF-SS(K)	$M^3 + (\mathcal{S} ^K + 4)M^2 + (\mathcal{S} ^K - 1)M$	$M^3 + (\mathcal{S} ^K + \frac{5}{2})M^2 + (\mathcal{S} ^K - \frac{7}{2})M - \mathcal{S} ^K$
MMSE-SS(K)	$\frac{3}{2}M^3 + (\mathcal{S} ^K + \frac{11}{2})M^2 + (\mathcal{S} ^K - 1)M$	$\frac{3}{2}M^3 + (\mathcal{S} ^K + 4)M^2 + (\mathcal{S} ^K - \frac{7}{2})M - \mathcal{S} ^K$
ZF-ES($L > 1$)	$M^3 + (\rho_1 + 5)M^2 + (\rho_1 + \frac{1}{2})M$	$M^3 + (\rho_1 + \frac{7}{2})M^2 + (\rho_1 - 1)M - \rho_1$
MMSE-ES($L > 1$)	$M^3 + (\rho_1 + 5)M^2 + (\rho_1 + \frac{1}{2})M$	$M^3 + (\rho_1 + \frac{7}{2})M^2 + \rho_1 M - \rho_1$
MMSE-ES($L > 1$)	$7M^3 + (\rho_L + 3)M^2 + (\rho_L - 1)M$	$7M^3 + (\rho_L + \frac{3}{2})M^2 + (\rho_L - \frac{3}{2})M - \rho_L$
MMSE-BLAST	$\frac{43}{12}M^4 + \frac{22}{3}M^3 + \frac{65}{12}M^2 - \frac{1}{3}M$	$\frac{43}{12}M^4 + \frac{20}{3}M^3 + \frac{53}{12}M^2 - \frac{5}{3}M$
ML	$ \mathcal{S} ^M M^2 + \mathcal{S} ^M M$	$ \mathcal{S} ^M M^2 + \mathcal{S} ^M M - \mathcal{S} ^M$


 Fig. 3. SER performance of MMSE-based MIMO detection schemes for 4×4 MIMO with 16-QAM.

 Fig. 4. SER performance of MMSE-based MIMO detection schemes for 4×4 MIMO with 64-QAM.

V. SIMULATION RESULTS AND DISCUSSIONS

Here, we present the performance and complexity of the considered detection schemes for different system settings. The symbol-error-rate (SER) performance is shown in Figs. 3–5 and the complexity is presented in Table II (in terms of floating-point operations or flops, where one complex multiplication counts six flops and one complex addition counts two flops). Since ZF- and MMSE-based schemes demonstrate consistent comparison results in our extensive simulation, here, we show only results for MMSE-based schemes. In Fig. 3, for a 4×4 MIMO system with 16-QAM, MMSE-ES(1), MMSE-ES(2), MMSE-ES(4), and MMSE-SS(1) all demonstrate a comparable 4-dB gain over the conventional MMSE detector at $\text{SER} = 10^{-2}$, suggesting that the use of additional dimensions in the ES method is not advantageous. In particular, even with the use of maximal $L = M = 4$, the “distortion effect” of the initial equalization that leads to degraded performance and loss of diversity gain [12] can still only be partially mitigated by post-equalization constellation search. MMSE-SS(2) has an 8-dB gain, and MMSE-BLAST has a 12-dB gain over the MMSE detector. The computational cost of MMSE-ES(1) is about twice of that of MMSE at high SNRs, which is significantly lower than that of MMSE-BLAST. The complexity of MMSE-SS quickly grows with each additional search subspace and with the order of modulation, rendering it more useful with $K = 1$ or $K = 2$ and for lower order modulations.

In Fig. 4, for a 4×4 MIMO system with 64-QAM, similar performance gains are observed. However, the MMSE-SS scheme loses its advantage in this case, as it is too computationally costly for


 Fig. 5. SER performance of MMSE-based MIMO detection schemes for 8×8 MIMO with 16-QAM.

the performance gain it provides. In contrast, the MMSE-ES scheme maintains its low complexity despite the higher order modulation. Similar conclusions about MMSE-SS and MMSE-ES can be drawn from Fig. 5 for an 8×8 system with 16-QAM. In this scenario, a more significant performance loss is observed for MMSE and the

TABLE II
COMPLEXITY COMPARISONS OF MIMO DETECTION SCHEMES IN TERMS OF NUMBER OF FLOPS FOR DIFFERENT SYSTEM SETTINGS

MIMO System	4×4						8×8					
	4-QAM		16-QAM		64-QAM		4-QAM		16-QAM		64-QAM	
SNR (dB)	18	32	24	44	30	50	24	38	30	50	36	56
ZF	804						5,352					
MMSE	812						5,368					
ZF-SS(1)	1,556		3,452		11,036		8,144		15,032		42,584	
ZF-SS(2)	3,452		41,372		648,092		15,032		152,792		2,356,952	
MMSE-SS(1)	2,004		3,900		11,484		10,960		17,848		45,400	
MMSE-SS(2)	3,900		41,820		648,540		17,848		155,608		2,359,768	
ZF-ES(1)	2,606	1,673	2,757	1,612	2,780	1,613	13,752	8,802	14,186	8,400	15,135	8,417
ZF-ES(2)	9,658	5,569	10,782	5,386	11,137	5,389	66,427	36,934	71,218	35,699	72,981	35,757
MMSE-ES(1)	2,614	1,681	2,765	1,620	2,788	1,621	13,768	8,818	14,202	8,416	15,151	8,433
MMSE-ES(2)	9,666	5,577	10,790	5,394	11,145	5,397	66,443	36,950	71,234	35,715	72,997	35,773
MMSE-BLAST	11,648						149,376					
ML	40,448		1.0×10^7		2.7×10^9		3.8×10^7		2.5×10^{12}		1.6×10^{17}	

proposed schemes compared with optimal ML detection. MMSE-ES(1) outperforms MMSE by about 4 dB at $SER = 10^{-2}$, and similar to previous scenarios, an increased search dimension does not provide an impressive performance gain for MMSE-ES. MMSE-BLAST achieves a higher gain over MMSE in this larger system but also at a higher complexity cost (about 30 times), as compared with that in a smaller system.

The overall performance and complexity results suggest that the proposed ES-based algorithms are particularly efficient for high operating SNRs and higher order modulations, and SS-based algorithms are useful for lower order modulations. In their suitable operating scenarios, both ES- and SS-based algorithms present very useful low-complexity options for MIMO detection.

VI. CONCLUSION

Two simple yet effective MIMO detection algorithms have been proposed. The proposed method consists of two phases, namely, standard linear detection and post-equalization constellation search in selected subspaces. Two algorithms conducting informed search in different subspaces associated with the largest estimation errors were proposed and compared. The demonstrated simplicity, low complexity, and performance make the proposed algorithms attractive for use in next-generation cellular systems such as LTE-A.

REFERENCES

- [1] Long Term Evolution Advanced (LTE-A). [Online]. Available: <http://www.3gpp.org/article/lte-advanced>
- [2] L. G. Barbero and J. S. Thompson, "Fixing the complexity of the sphere decoder for MIMO detection," *IEEE Trans. Wireless Commun.*, vol. 7, no. 6, pp. 2131–2142, Jun. 2008.
- [3] M. O. Damen, H. El Gamal, and G. Caire, "On maximum-likelihood detection and the search for the closest lattice point," *IEEE Trans. Inf. Theory*, vol. 49, no. 10, pp. 2389–2402, Oct. 2003.
- [4] B. Hassibi and H. Vikalo, "On the sphere-decoding algorithm I. Expected complexity," *IEEE Trans. Signal Process.*, vol. 53, no. 8, pp. 2806–2818, Aug. 2005.
- [5] B. Shim, J. W. Choi, and I. Kang, "Towards the performance of ML and the complexity of MMSE—A hybrid approach," in *Proc. IEEE GLOBECOM*, Dec. 2008, pp. 1–5.
- [6] D. Wübben, R. Böhnke, V. Kühn, and K.-D. Kammeyer, "Near-maximum-likelihood detection of MIMO systems using MMSE-based lattice reduction," in *Proc. IEEE ICC*, Jun. 2004, pp. 798–802.
- [7] T.-H. Liu and Y.-L. Liu, "Modified fast recursive algorithm for efficient MMSE-SIC detection of the V-BLAST system," *IEEE Trans. Wireless Commun.*, vol. 7, no. 10, pp. 3713–3717, Oct. 2008.
- [8] R. Böhnke, D. Wübben, V. Kühn, and K.-D. Kammeyer, "Reduced complexity MMSE detection for BLAST architectures," in *Proc. IEEE GLOBECOM*, Dec. 2003, pp. 2258–2262.
- [9] N. Al-Dhahir, A. F. Naguib, and A. R. Calderbank, "Finite-length MIMO decision feedback equalization for space-time block-coded signals over multipath-fading channels," *IEEE Trans. Veh. Technol.*, vol. 50, no. 4, pp. 1176–1182, Jul. 2001.
- [10] J. W. Choi, B. Shim, A. C. Singer, and N. I. Cho, "Low-complexity decoding via reduced dimension maximum-likelihood search," *IEEE Trans. Signal Process.*, vol. 58, no. 3, pp. 1780–1793, Mar. 2010.
- [11] T. Abe and T. Matsumoto, "Space-time turbo equalization in frequency-selective MIMO channels," *IEEE Trans. Veh. Technol.*, vol. 52, no. 3, pp. 469–475, May 2003.
- [12] H. Artés, D. Seethaler, and F. Hlawatsch, "Efficient detection algorithms for MIMO channels: A geometrical approach to approximate ML detection," *IEEE Trans. Signal Process.*, vol. 51, no. 11, pp. 2808–2820, Nov. 2003.
- [13] G. H. Golub and C. F. Van Loan, *Matrix Computations*, 3rd ed. Baltimore, MD: Johns Hopkins Univ. Press, 1996.
- [14] S. M. Kay, *Fundamentals of Statistical Signal Processing: Estimation Theory*. Englewood Cliffs, NJ: Prentice-Hall, 1993.
- [15] A. Edelman, "Eigenvalues and condition numbers of random matrices," Ph.D. dissertation, MIT, Cambridge, MA, 1989.
- [16] I. Dimov and A. Karaivanova, "A power method with Monte Carlo iterations," in *Recent Advances in Numerical Methods and Applications*. Singapore: World Scientific, 1999, pp. 239–247.
- [17] P. W. Wolniansky, G. J. Foschini, G. D. Golden, and R. A. Valenzuela, "V-BLAST: An architecture for realizing very high data rates over the rich-scattering wireless channel," in *Proc. ISSSE*, Sep. 1998, pp. 295–300.
- [18] J. Benesty, Y. Huang, and J. Chen, "A fast recursive algorithm for optimum sequential signal detection in a BLAST system," *IEEE Trans. Signal Process.*, vol. 51, no. 7, pp. 1722–1730, Jul. 2003.